JCB Article

Zinc and the Msc2 zinc transporter protein are required for endoplasmic reticulum function

Charissa D. Ellis,[1] Fudi Wang,[2] Colin W. MacDiarmid,[1] Suzanne Clark,[2] Thomas Lyons,[1] and David J. Eide[1,2]

[1]Department of Biochemistry and [2]Department of Nutritional Sciences, University of Missouri, Columbia, MO 65211

In this report, we show that zinc is required for endoplasmic reticulum function in *Saccharomyces cerevisiae*. Zinc deficiency in this yeast induces the unfolded protein response (UPR), a system normally activated by unfolded ER proteins. Msc2, a member of the cation diffusion facilitator (CDF) family of metal ion transporters, was previously implicated in zinc homeostasis. Our results indicate that Msc2 is one route of zinc entry into the ER. Msc2 localizes to the ER when expressed at normal levels. UPR induction in low zinc is exacerbated in an *msc2* mutant. Genetic and biochemical evidence indicates that this UPR induction is due to genuine ER dysfunction. Notably, we found that ER-associated protein degradation is defective in zinc-limited *msc2* mutants. We also show that the vacuolar CDF proteins Zrc1 and Cot1 are other pathways of ER zinc acquisition. Finally, zinc deficiency up-regulates the mammalian ER stress response indicating a conserved requirement for zinc in ER function among eukaryotes.

Introduction

Zinc is an important cofactor for many proteins that reside in or pass through organelles of the secretory system. For example, packaging of insulin in secretory granules of pancreatic β-cells is dependent on Zn^{2+} (Huang and Arvan, 1995; Dodson and Steiner, 1998). Matrix metalloproteases are Zn^{2+}-requiring enzymes that are secreted by cells to modify the ECM during development and tumor cell metastasis (Chang and Werb, 2001). These proteins acquire zinc at an early point in the secretory pathway (Pei and Weiss, 1995; Kang et al., 2002). Addition of phosphoethanolamine groups to glycosylphosphatidylinositol (GPI) anchors requires Zn^{2+}-dependent enzymes in the ER (Galperin and Jedrzejas, 2001; Mann and Sevlever, 2001; Sevlever et al., 2001). As a last example, some protein chaperones homologous to *Escherichia coli* DnaJ, like the ER-localized Scj1 of *Saccharomyces cerevisiae*, likely require Zn^{2+} to function in protein folding and in the degradation of misfolded proteins by quality control mechanisms (Silberstein et al., 1998; Nishikawa et al., 2001; Tang and Wang, 2001; Linke et al., 2003). These many requirements for Zn^{2+} in the secretory pathway highlight the need for zinc transporters to deliver the metal to those organelles. Despite the importance of these various zinc-dependent processes in normal cell function and disease states such as cancer, the transport proteins responsible for zinc delivery have not yet been identified.

Members of the cation diffusion facilitator (CDF) family of transport proteins are likely candidates to transport Zn^{2+} into the secretory pathway. CDF proteins play conserved roles in transporting Zn^{2+} from the cytosol into organelles or out of the cell in many organisms (Nies and Silver, 1995; Paulsen and Saier, 1997; Gaither and Eide, 2001; Palmiter and Huang, 2004). In *E. coli*, for example, the ZitB CDF protein transports excess zinc from the cytosol to the extracellular environment (Grass et al., 2001). In mammals, ZnT-1 similarly transports excess cytosolic zinc, whereas ZnT-2 may detoxify the metal by sequestering it in the late endosome (Palmiter and Findley, 1995; Palmiter et al., 1996; Kobayashi et al., 1999). Three mammalian CDF proteins implicated in Zn^{2+} transport into the secretory pathway are ZnT-5, ZnT-6, and ZnT-7, each of which having been localized to the Golgi apparatus (Huang et al., 2002;

Address correspondence to David J. Eide, Dept. of Nutritional Sciences, 217 Gwynn Hall, University of Missouri, Columbia, MO 65211. Tel.: (573) 882-9686. Fax: (573) 882-0185. email: eided@missouri.edu

C.W. MacDiarmid's present address is R424 Research Building, Dept. of Biology, University of Missouri-St. Louis, One University Blvd., St. Louis, MO 63121-4499.

S. Clark's present address is F032A, 800 Hospital Dr., Dept. of Medicine-Endocrinology University of Missouri-Columbia, Columbia, MO 65211.

T. Lyons' present address is 404 Leigh Hall, Dept. of Chemistry, University of Florida, 127 Chemistry Research Building, P.O. Box 117200, Gainesville, FL 32611-7200.

Key words: zinc; transport; cation diffusion facilitator; endoplasmic reticulum; unfolded protein response

Abbreviations used in this paper: CDF, cation diffusion facilitator; ERAD, ER-associated degradation; GPI, glycosylphosphatidylinositol; TPEN, N,N,N′,N′-tetrakis-(2-pyridyl-methyl)ethylenediamine; UPR, unfolded protein response; ZRE, zinc-responsive element.

The Journal of Cell Biology, Volume 166, Number 3, August 2, 2004 325–335
http://www.jcb.org/cgi/doi/10.1083/jcb.200401157

Kambe et al., 2002; Kirschke and Huang, 2003). The functional roles of these proteins are not yet clear.

We have learned much about zinc homeostasis from studies of the yeast *S. cerevisiae*. In this yeast, zinc uptake is mediated by the high affinity Zrt1 transporter and the lower affinity Zrt2 and Fet4 proteins (Zhao and Eide, 1996a, 1996b; Waters and Eide, 2002). The genes encoding these transporters are controlled by the Zap1 transcriptional activator protein (Zhao and Eide, 1997). Zap1 is active in zinc-limited cells and its activity is repressed in zinc-replete cells. Zap1 binds to one or more zinc-responsive elements (ZREs) in the promoters of its target genes (Zhao et al., 1998).

Zinc storage and detoxification in *S. cerevisiae* is mediated by the vacuole. The Zrc1 and Cot1 proteins, both members of the CDF family, are responsible for zinc transport into the vacuole (Kamizono et al., 1989; MacDiarmid et al., 2000, 2002; Miyabe et al., 2001). Two other CDF proteins, Mmt1 and Mmt2, have been implicated in iron transport in the mitochondria (Li and Kaplan, 1997). The fifth yeast CDF member, and the subject of this report, is Msc2. Msc2 was first identified in a screen for mutations with altered frequencies of meiotic sister chromatid exchange (Thompson and Stahl, 1999). However, the link between DNA recombination and the *MSC2* gene is unclear; the effects on recombination are allele specific and not observed in a full *msc2* deletion mutant (Thompson and Stahl, 1999). A more recent study of Msc2 suggested that it played some role in zinc metabolism (Li and Kaplan, 2000). An *msc2* mutant grew poorly on respired carbon sources at elevated temperatures and had an abnormally large cell size. Both of these phenotypes were suppressed by addition of excess zinc. In this report, we demonstrate that Msc2 is an ER membrane protein whose role is to maintain proper function of the ER. Our results indicate that key processes in the ER require Zn^{2+} and that Msc2 is involved in supplying Zn^{2+} to this compartment.

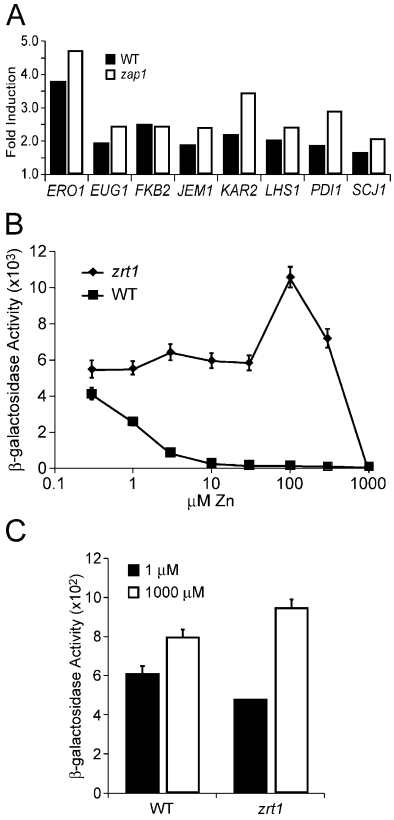

Figure 1. **Zinc deficiency induces the UPR.** (A) Microarray analysis of UPR target genes showing greater than or equal to twofold induction in low zinc over high zinc in both wild-type and *zap1* mutant cells. These data are from experiments described previously (Lyons et al., 2000). (B) UPRE-*lacZ* activity in wild type (WT, DY1457) and the *zrt1* mutant (ZHY1) over a range of zinc concentrations in LZM. LZM is zinc limiting because 1 mM EDTA is added to limit metal availability. Shown are representative data from two experiments. (C) *HIS4-lacZ* activity in DY1457 and ZHY1 in low (1 μM) and high (1,000 μM) zinc in LZM. Shown are representative data from two experiments. The error bars indicate ± 1 SD.

Results

Zinc deficiency induces the unfolded protein response (UPR)

Genome-wide cDNA microarray analysis of gene expression in *S. cerevisiae* indicated that many genes (458) are induced by zinc deficiency (Lyons et al., 2000). This included 46 direct Zap1 targets and 412 genes up-regulated in a Zap1-independent fashion. Induction of this latter group probably reflects indirect effects of zinc deficiency on cell function. Among the genes indirectly affected by zinc were several involved in the UPR. The UPR is a response to the accumulation of unfolded proteins in the ER (Patil and Walter, 2001). Fig. 1 A summarizes the microarray results for eight genes of the UPR (Travers et al., 2000) that were up-regulated by twofold or more in zinc-deficient wild-type cells. The up-regulation of these genes is independent of Zap1; each showed similar induction by zinc deficiency in a *zap1* mutant. The UPR genes induced by zinc deficiency include *ERO1*, *EUG1*, and *PDI1* (encoding proteins involved in protein disulfide isomerization) and *FKB2* (encoding peptidyl-prolyl cis-trans isomerase). In addition, *JEM1*, *KAR2*, *LHS1*, and *SCJ1* were also up-regulated. These genes encode ER chaperones that facilitate the translocation of misfolded ER proteins back to the cytosol for degradation in a process known as ER-associated degradation (ERAD).

These data indicated that zinc deficiency up-regulates the UPR. To confirm this hypothesis, we used a UPR-responsive reporter gene to assess the effect of zinc deficiency on UPR induction. UPR target genes contain UPRE sequences in their promoters that confer this regulation. A UPRE-*lacZ* reporter was highly induced in wild-type cells grown in low zinc (Fig. 1 B, LZM + 0.3 μM Zn) relative to zinc-replete cells (Fig. 1 B, LZM + 1,000 μM Zn). These experiments were performed using LZM medium which is zinc-limiting due to addition of 1 mM EDTA. Adding as little as 10 μM $ZnCl_2$ to LZM was sufficient to repress UPRE-*lacZ* expression. UPRE-*lacZ* induction in low zinc was also observed in *zrt1* mutants defective for zinc uptake. Because Zrt1 is the major zinc uptake transporter in yeast, the *zrt1* mutant is zinc deficient when grown in LZM supplemented with ≤300 μM $ZnCl_2$ (Zhao and Eide, 1996a). The UPRE-*lacZ* reporter showed high levels of β-galactosidase activity in the *zrt1* mutant over a wide range of zinc concentrations and

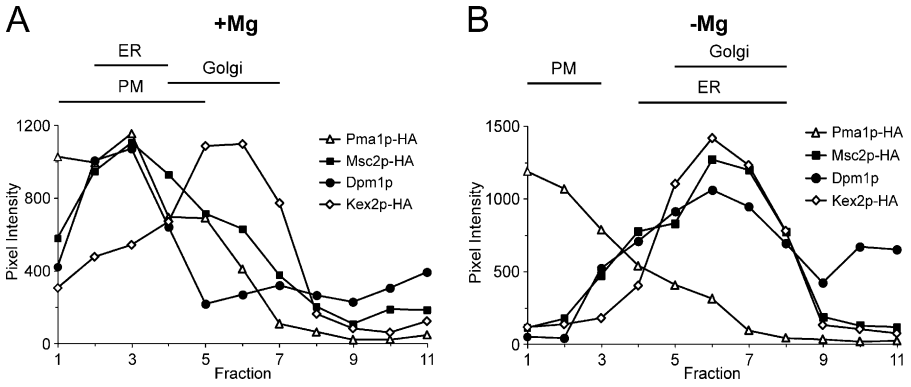

Figure 2. **Msc2 is localized to the endoplasmic reticulum.** Lysates were prepared from wild-type (WT, DY150) cells expressing either pMSC2HA and pSN222 (Kex2-HA) or pGEV-TRP and pRK315 (Pma1-HA). Extracts were layered onto sucrose gradients for subcellular fractionation. Gradient fractions were subjected to immunoblotting and probed with anti-HA or anti-Dpm1 antibodies. Fractions are numbered from 1 (heaviest) to 11 (lightest). Shown are representative data from three experiments. (A) Plot of immunoblot band intensities from fractions prepared +Mg. (B) Plot of immunoblot band intensities from fractions processed −Mg. The lines labeled ER, PM, and Golgi denote fractions containing ≥50% of the peak values for the corresponding marker protein.

was suppressed only by adding 1,000 μM zinc to the media (Fig. 1 B). A *HIS4-lacZ* control reporter, which is not responsive to either zinc or unfolded proteins, showed high expression in both the wild-type and the *zrt1* mutant strains at all zinc concentrations (Fig. 1 C). Therefore, the effects seen with the UPRE-*lacZ* reporter are specific UPR effects and not general effects on β-galactosidase activity. The twofold increase in UPRE-*lacZ* expression observed between 30 and 100 μM zinc (Fig. 1 A) is similar to that seen with other promoters (Fig. 1 C, *HIS4-lacZ*) and probably reflects a general decrease in expression in severely zinc-deficient cells.

Msc2 localizes to the ER

Induction of the UPR in low zinc suggested that zinc transport into the lumen of the ER is required for ER function. A transporter protein possibly involved in delivering zinc into the ER is encoded by the *MSC2* gene. Previous studies suggested that Msc2 was localized to the endoplasmic reticulum. However, these experiments were done under conditions where Msc2 was overexpressed. Because overexpression can result in protein mislocalization, the true intracellular location of Msc2 was unclear. Therefore, we determined the localization of Msc2 when expressed from its own promoter on a low copy plasmid. To aid detection of Msc2, we generated an *MSC2* allele with three HA tags fused to its COOH terminus. Immunoblots detected only a single band near the predicted molecular mass of Msc2 (unpublished data). Moreover, the epitope-tagged protein complemented the temperature-sensitive growth defect phenotype of an *msc2* mutant strain indicating that it is functional.

Attempts to determine the subcellular localization of Msc2 using immunofluorescence microscopy were inconclusive because the level of expression was too low. Therefore, we used sucrose gradient fractionation to assess the distribution of Msc2. Protein extracts of wild-type cells expressing HA-tagged Msc2 were separated on sucrose gradients. After centrifugation, fractions were collected and analyzed by immunoblotting. Previous reports have shown that the presence or absence of Mg^{2+} greatly alters the position of ER vesicles in the gradient (Roberg et al., 1997). Without added Mg^{2+}, the ER colocalizes with the Golgi apparatus in the middle fractions of the gradient. However, in the presence of Mg^{2+}, the ER localizes to the heavier fractions of the gradient, colocalizing with the plasma membrane. This shift to heavier fractions is likely due to ribosomes remaining associated with the ER when Mg^{2+} is present. If Msc2 localizes to the ER, we predicted that the protein would show this Mg^{2+}-dependent shift in these gradients.

Kex2 is a Golgi marker protein and its localization, peaking around fraction 6 in the middle of the gradients (Fig. 2), was unaffected by Mg^{2+}. A plasma membrane protein, Pma1, also was largely unaffected by Mg^{2+} levels with its peak localization in the heaviest fractions of both gradients. Dpm1 served as an ER marker. Both Msc2 and Dpm1 showed the diagnostic ER Mg^{2+} shift being found in the heavier fractions with Mg^{2+} and localizing in the middle fractions without Mg^{2+}. Because Msc2 colocalizes with an ER marker protein and shows the characteristic ER Mg^{2+} shift, these studies strongly support the localization of Msc2 to that compartment. In the presence of Mg^{2+}, some Msc2 was also found in lighter fractions that may correspond to the Golgi. Little Dpm1 was found in these lighter fractions.

Mutation of MSC2 alters zinc homeostasis

If Msc2 transports zinc into the ER lumen, we predicted that mutation of the *MSC2* gene would alter homeostasis of cytosolic labile zinc. A useful bioassay of this labile zinc is the Zap1 transcription factor, which binds to ZREs in it target promoters. Zap1 is active in zinc-limited cells and repressed by high zinc. The zinc response curve of a ZRE-*lacZ* reporter in wild-type cells is shown in Fig. 3 A. If Msc2 transported zinc into the ER, we predicted that cytosolic zinc levels would increase in an *msc2* mutant strain and repress Zap1 activity. Consistent with this prediction, expression of the ZRE-*lacZ* reporter was suppressed in *msc2* cells grown in LZM + 0.3–10 μM $ZnCl_2$ (Fig. 3 A). Mutation of *MSC2* did not decrease expression of the *HIS4-lacZ* reporter indicating that the effects of the *msc2* mutation were specific to the ZRE-*lacZ* reporter (Fig. 3 B). These results suggest that Msc2 transports zinc from the cytosol into the ER lumen.

Effects of msc2 mutation on UPR induction

If Msc2 transports zinc into the ER, we predicted that an *msc2* mutant would increase induction of the UPR in low

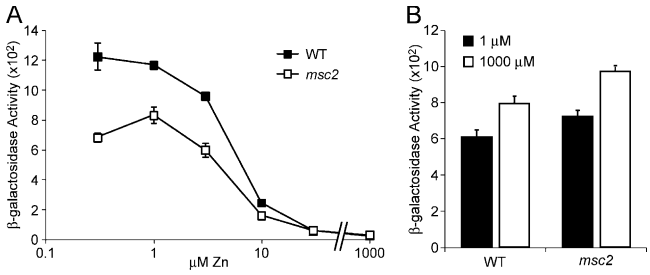

Figure 3. **The *msc2* mutation increases labile zinc levels.** (A) ZRE-*lacZ* activity in wild type (WT, DY150) and the *msc2* mutant (DY150 *msc2*) grown over a range of zinc concentrations in LZM. Shown are representative data from five experiments. (B) *HIS4-lacZ* activity in wild type (WT, DY150) and the *msc2* mutant (DY150 *msc2*) in low (1 μM) and high (1,000 μM) zinc in LZM. Shown are representative data from five experiments. The error bars indicate ± 1 SD.

zinc relative to wild-type cells. This prediction was confirmed using the UPRE-*lacZ* reporter (Fig. 4 A). Although the wild-type strain showed some induction of the UPR in low zinc, this up-regulation was substantially increased in the *msc2* mutant strain. These data suggest that a strain lacking *MSC2* experiences greater ER stress when coupled with zinc deficiency. To determine the metal specificity of this effect, we measured UPRE-*lacZ* expression in an *msc2* mutant under low zinc conditions when higher levels of zinc or other metals were added. Although as little as 10 μM zinc suppressed the UPR up-regulation, neither 10 nor 100 μM of Fe^{2+}, Cu^{2+}, Cd^{2+}, Mn^{2+}, Ni^{2+}, or Co^{2+} greatly suppressed this up-regulation (Fig. 4 B). Therefore, UPR induction in an *msc2* mutant is a zinc-specific effect.

UPRE-lacZ induction by low zinc and msc2 mutation requires a functioning UPR signaling pathway

UPR induction is achieved through a two-protein signaling pathway (for review see Patil and Walter, 2001). Ire1 is a transmembrane endo-RNase protein that senses unfolded proteins in the ER. Hac1 is the transcription factor that responds to that signal to increase expression of UPR target genes. When Ire1 is activated by unfolded ER proteins, it cleaves an intron out of the *HAC1* mRNA. The spliced *HAC1* mRNA is translated into protein ($Hac1^i$), which then up-regulates UPR target genes. To verify that the induction of the UPR in an *msc2* mutant is dependent on the Ire1–Hac1 signaling pathway, we constructed *msc2 ire1* and *msc2 hac1* double mutants and analyzed their UPRE-*lacZ* activity. DTT, a known inducer of the UPR because of its ability to disrupt disulfide bonds in ER proteins, did not cause UPRE-*lacZ* induction in *ire1* and *hac1* mutants in both the wild-type and the *msc2* mutant backgrounds (unpublished data). These mutants were also impaired for induction of the UPR in low zinc (Fig. 5 A). These strains had no such effect on the control *HIS4-lacZ* reporter (not depicted). Therefore, the induction of the UPR in low zinc in an *msc2* mutant requires the full UPR signaling pathway.

One can also envisage that an *msc2* mutant may somehow hyperactivate $Hac1^i$ independently of Ire1. To test this hypothesis, we introduced an intron-less form of the *HAC1* gene on a low copy plasmid ($pHac1^i$) into both wild-type and *msc2* mutant strains. This plasmid-encoded $Hac1^i$ does not

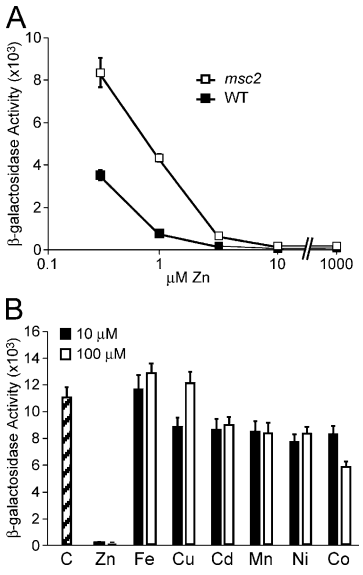

Figure 4. **The *msc2* mutant increases UPR induction in zinc deficiency.** (A) UPRE-*lacZ* activity in wild-type (WT, DY150) and the *msc2* mutant (DY150 *msc2*) over a range of zinc concentrations in LZM. Shown are representative data from three experiments. (B) UPRE-*lacZ* activity in the *msc2* mutant in LZM + 0.3 μM Zn. The control condition, C, had no added metals. Shown are representative data from two experiments. The error bars indicate ± 1 SD.

rely on Ire1 for its activation, and therefore causes constitutive UPR induction. We predicted that if the *msc2* mutation made endogenous $Hac1^i$ more active, it would have a similar effect on plasmid-encoded $Hac1^i$. This was not the case. Introduction of $pHAC1^i$ into wild-type cells actually caused

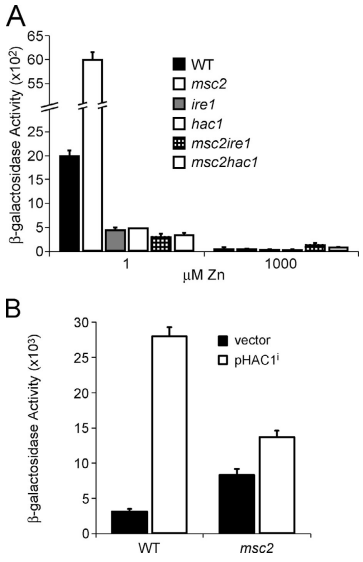

Figure 5. **The *msc2* mutant requires Ire1 and Hac1 for UPR induction.** (A) UPRE-*lacZ* activity in wild type (WT, DY150), *msc2* (DY150 *msc2*), *ire1* (CEY3), *hac1* (CEY4), *msc2 ire1* (CEY5), and *msc2 hac1* (CEY6) in low (1 μM) and high (1,000 μM) zinc in LZM. Shown are representative data from three experiments. (B) UPRE-*lacZ* activity in wild type (WT, DY150) and the *msc2* mutant (DY150 *msc2*) expressing vector (pRS315) or $pHAC1^i$ in low (1 μM) zinc in LZM. Shown are representative data from five experiments. The error bars indicate ± 1 SD.

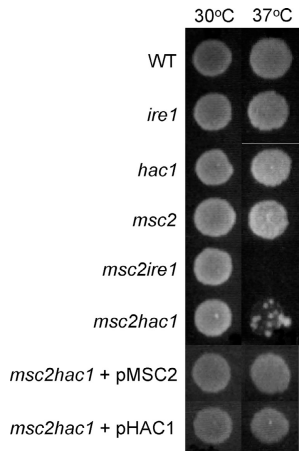

Figure 6. **The *msc2* mutant is synthetically lethal with *ire1* and *hac1* at elevated temperatures.** Yeast cells were grown in YPD or SD liquid medium overnight. Cultures were diluted in fresh media and 5 μl vol (10^4 cells) were plated onto YPD plates, incubated at 30 or 37°C, and photographed after 2 d. Wild type (WT, DY150), *msc2* (DY150 *msc2*), *ire1* (CEY3), *hac1* (CEY4), *msc2 ire1* (CEY5), and *msc2 hac1* (CEY6) were grown and diluted in YPD before plating; *msc2 hac1* + pMSC2 and *msc2 hac1* + pHAC1 were grown and diluted in SD before plating.

higher levels of UPRE-*lacZ* activity than was observed in the *msc2* mutant (Fig. 5 B). Although the reason for the decreased expression in the mutant is not yet known, this result clearly demonstrates that the *msc2* mutation does not increase Hac1^i activity independently of the UPR signaling pathway.

Genetic and biochemical evidence for ER dysfunction in msc2 mutants

The requirement for an intact Ire1–Hac1 signaling pathway to induce the UPR in response to low zinc and loss of Msc2 function suggested that these factors perturbed ER function. Further evidence supporting this conclusion came from the observation that *msc2 ire1* and *msc2 hac1* mutants exhibit a synthetic lethal growth phenotype. *msc2* single mutants grow poorly at 37°C on YP medium supplemented with glycerol and ethanol, two nonfermentable carbon sources, but show no such defect on media supplemented with glucose (YPD), a fermentable carbon source (Fig. 6). Similarly, neither *ire1* nor *hac1* mutants exhibit a growth defect on YPD at either 30 or 37°C. Combining these mutations, i.e., *msc2 ire1* and *msc2 hac1*, resulted in a strong growth defect at 37°C. (The few colonies seen in the *msc2 hac1* mutant at 37°C may be the result of spontaneously arising suppressor mutations. More than 99% of the inoculated *msc2 hac1* cells failed to grow at the elevated temperature.) Introducing the *MSC2* or *HAC1* genes on low copy plasmids (pMSC2, pHAC1) back into the *msc2 hac1* mutant restored growth at 37°C. Thus, an *msc2* mutant requires both Ire1 and Hac1 to survive at higher temperatures.

To further test the hypothesis that *msc2* mutation and low zinc causes ER dysfunction, we examined one aspect of ER function, degradation of unfolded proteins through the ERAD pathway. This particular aspect was addressed because Scj1, an ER lumenal chaperone required for ERAD function, has two predicted zinc binding sites and is likely to require zinc for its activity. The homologous *E. coli* DnaJ protein was shown to be zinc dependent (Tang and Wang, 2001; Linke et al., 2003). A useful assay of the ERAD system is to monitor the degradation of CPY*, a mutant carboxypeptidase Y protein that fails to fold properly and is degraded by ERAD (Finger et al., 1993). Wild-type and *msc2* mutants were transformed with a plasmid expressing CPY* bearing an HA epitope tag (Ng et al., 2000). The cells were grown in high or low zinc and then treated with cycloheximide to block further protein synthesis. Aliquots were removed periodically over 60 min for protein extraction and immunoblotting. No difference was observed between wild-type and *msc2* mutants in either growth condition (unpublished data).

The UPR system induces expression of Scj1 and a second, partially redundant chaperone called Jem1 (Fig. 1; Nishikawa and Endo, 1997). Although Scj1 is probably zinc dependent, Jem1 lacks the zinc-binding sites and is therefore likely to be zinc independent. Therefore, increased expression of the Jem1 chaperone may compensate for the loss of zinc-dependent Scj1 activity. To test this hypothesis, we examined CPY* degradation in *jem1* mutant cells lacking the zinc-independent chaperone. CPY* turnover in a *jem1* single mutant was rapid in both zinc-limited and replete cells (Fig. 7). CPY* degradation in zinc-replete *jem1 msc2* mutants was indistinguishable from the *jem1* single mutant. However, the *jem1 msc2* mutant showed a marked defect in CPY* degradation in low zinc.

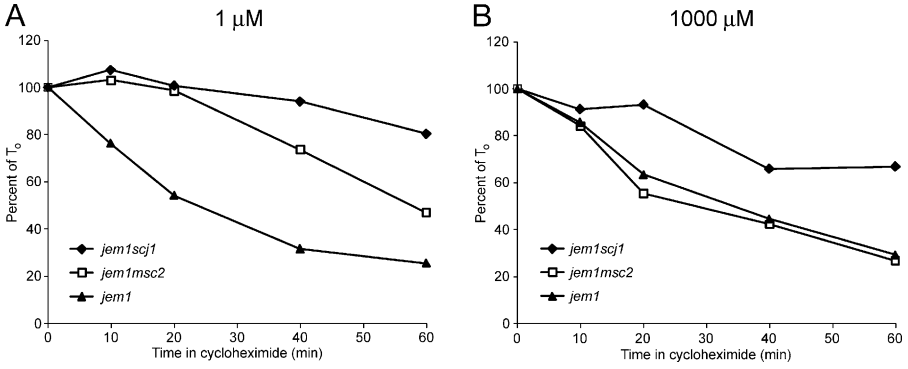

Figure 7. **The *msc2* mutant has defects in ERAD in low zinc.** LZM cultures of *jem1* (CEY13), *jem1 msc2* (CM164), and *jem1 scj1* (CEY17) expressing the CPY*–HA plasmid (pDN436U) were grown in the presence of cycloheximide for 0–60 min before protein extraction. Extracts were analyzed by immunoblotting using mouse anti-HA or mouse anti-Pgk1 antibodies. The intensities of the CPY*–HA bands were normalized to the Pgk1 bands. Each time point was then calculated as the percentage of the zero time point (T_o) for that strain. Shown are the averages of four experiments. (A) Plot of percent of T_o for cultures grown in low (1 μM) zinc in LZM. (B) Plot of percent of T_o for cultures grown in high (1,000 μM) zinc in LZM.

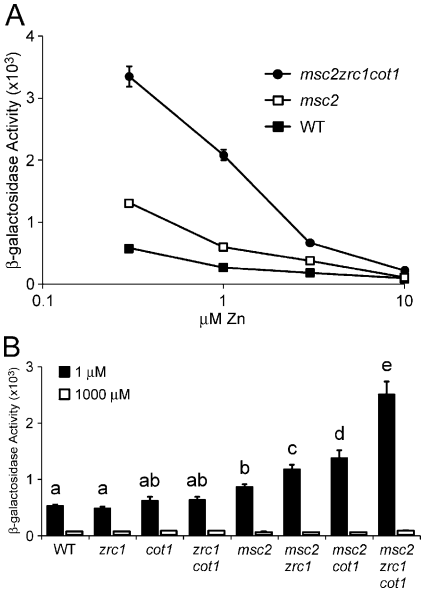

Figure 8. **Zrc1 and Cot1 may also transport zinc into the ER.** (A) UPRE-*lacZ* activity in wild type (WT, CM100), *msc2* (CEY7), and *msc2 zrc1 cot1* (CEY8) over a range of zinc concentrations in LZM. Cells were grown in LZM + 10 μM Zn to deplete internal zinc stores before inoculation. Shown are representative data from three experiments. (B) UPRE-*lacZ* activity in cells grown in low (1 μM) and high (1,000 μM) zinc in LZM: wild type (WT, CM100), *zrc1* (CM102), *cot1* (CM103), *zrc1 cot1* (CM104), *msc2* (CEY7), *msc2 zrc1* (averages of CEY19-21), *msc2 cot1* (averages of CEY22, 23), and *msc2 zrc1 cot1* (averages of CEY8, CEY27-29). Shown are data from one representative experiment done in triplicate. Letters refer to values that are significantly different from each other, as determined using the Scheffe's test, with $P < 0.05$. The error bars indicate ± 1 SD.

These studies indicate that zinc deficiency impairs function of components, likely Scj1, of the ERAD system. Consistent with this hypothesis, CPY* degradation was defective in a *jem1 scj1* double mutant at both zinc levels (Fig. 7).

Zrc1 and Cot1 also contribute to ER zinc

The ability of elevated zinc to suppress UPRE-*lacZ* induction in an *msc2* mutant (Fig. 4 A) indicated that other transporters in addition to Msc2 may also provide zinc to the ER. Two possible candidates for this role are Zrc1 and Cot1, members of the CDF protein family that transport zinc into the vacuole. Although the steady-state location of these proteins is the vacuole membrane, they must transit through the ER en route to that compartment. Therefore, we tested the contribution of Zrc1 and Cot1 to ER function using the UPRE-*lacZ* reporter. Consistent with Zrc1 and/or Cot1 also contributing to ER zinc, induction of the UPRE-*lacZ* reporter was greatly increased in a zinc-deficient *msc2 zrc1 cot1* triple mutant relative to an *msc2* mutant or wild-type cells (Fig. 8 A). To determine if either or both Zrc1 and Cot1 were involved, we generated a series of single and double mutants and assayed their effects on UPRE-*lacZ* induction in low zinc and high zinc. In high zinc, all strains tested exhibited no UPRE-*lacZ* induction (Fig. 8 B). Under zinc-deficient conditions, *zrc1*, *cot1*, and *zrc1 cot1* cells showed UPR induction indistinguishable from wild-type cells. Zinc-deficient *msc2* mutant cells had increased UPRE-*lacZ* expression that was further increased in the *msc2 zrc1* and *msc2 cot1* mutants. Finally, UPRE-*lacZ* induction was highest in the *msc2 zrc1 cot1* mutant. These results suggested that all three transporters contribute to ER function.

Zinc deficiency induces the UPR in mammalian cells

Finally, we addressed if the effects of zinc deficiency on the UPR was evolutionarily conserved. In mammals, ATF6 is a member of the basic-leucine zipper family of transcription factors that acts analogously to yeast Hac1 to control the UPR (for review see Harding et al., 2002). ATF6 contains a transmembrane domain and is localized to the ER membrane. Upon ER stress, ATF6 is proteolytically cleaved to release the NH_2-terminal b-Zip–containing domain which then translocates into the nucleus to activate UPR gene expression. To address if zinc deficiency activates the UPR in mammalian cells, we examined the effects of zinc deficiency on expression of an ATF6-responsive reporter plasmid (p5xATF6GL3; Wang et al., 2000) transiently transfected into HeLa cells. p5xATF6GL3 contains five copies of the ATF6 binding site inserted upstream of the firefly luciferase gene. These cells were cotransfected with a *lacZ* gene driven by the SV40 promoter to normalize for differences in transfection efficiency. As shown in Fig. 9 A, treating HeLa cells bearing p5xATF6GL3 with tunicamycin, a glycosylation inhibitor and known inducer of ATF6 activity, resulted in a marked induction of luciferase expression. To induce zinc deficiency, cells were treated with 5 μM of the zinc chelator N,N,N′,N′-tetrakis-(2-pyridyl-methyl)ethylenediamine (TPEN). Cells were then harvested over a 12-h period and assayed for luciferase expression. After 5 h of TPEN treatment, a small increase in luciferase activity was observed (Fig. 9 B). After 12 h, luciferase activity was induced approximately fourfold. No loss of cell viability was detected over this 12-h period (unpublished data) indicating that the induction was not due to necrosis or apoptosis. To determine the concentration of TPEN optimal to triggering UPR induction, we assayed the effects of a range of TPEN concentrations after a 12-h treatment. TPEN concentrations of ≤ 3 μM had no effect on ATF6 activity whereas concentrations of 4 or 5 μM induced expression above basal levels (Fig. 9 C). Finally, we addressed if the effects of TPEN on UPR induction were due to zinc deficiency or a pharmacological effect of TPEN. Consistent with zinc deficiency being the cause, simultaneous incubation of cells with 5 μM TPEN and 5 μM $ZnCl_2$ failed to induce ATF6 activity (Fig. 9 D). These results suggest that the requirement of the ER for zinc is evolutionarily conserved and that zinc deficiency induces the UPR in a wide range of organisms.

Discussion

In a previous report, Li and Kaplan (2000) proposed that Msc2 transports zinc out of the nucleus into the cytosol. This hypothesis was based on the tentative localization of overexpressed Msc2 to the nuclear envelope (which is contiguous with the ER membrane) and the observation that the Zap1 transcription factor was completely repressed under their zinc-deficient conditions in an *msc2* mutant. We questioned this hypothesis because the relatively large size of

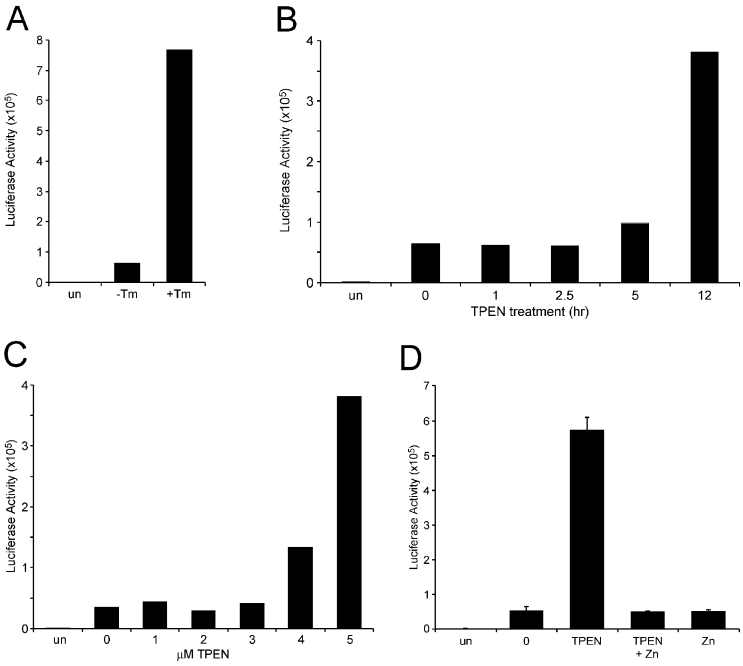

Figure 9. **Zinc deficiency induces the mammalian ER stress response.** HeLa cells were transiently transfected with pSV-β-galactosidase and p5xATF6GL3 plasmids. Cells were then subjected to different treatments, protein was extracted, and β-galactosidase and luciferase assays performed. Luminometer readings were normalized to β-galactosidase activity values to adjust for differences in transfection efficiencies. In all experiments, "un" refers to untransfected cells. (A) Luciferase activity in cells treated with (+Tm) and without (−Tm) tunicamycin (12 h, 2 μM tunicamycin). (B) Time course of luciferase activity for cells treated with 5 μM TPEN for 0, 1, 2.5, 5, or 12 h. (C) Concentration response of luciferase activity for cells treated with 0, 1, 2, 3, 4, or 5 μM TPEN for 12 h. (D) Luciferase activity in cells with different 12-h treatments: no treatment (0), 5 μM TPEN (TPEN), 5 μM TPEN and 5 μM Zn (TPEN+Zn), or 5 μM Zn (Zn). The error bars indicate ± 1 SD.

the nuclear pore is unlikely to limit diffusion of Zn^{2+} ions between the cytosol and the nucleus (Shulga et al., 2000). In this report, we propose the alternative model that zinc is required for ER function and Msc2 transports the metal into the ER lumen.

Several lines of evidence support the hypothesis that Msc2 is involved in zinc metabolism. First, Msc2 is a member of the CDF family of metal ion transporters. Studies of CDF proteins in many organisms have established that these proteins transport their metal ion substrate, usually Zn^{2+}, from the cytosol to either outside of the cell or into organelles (Nies and Silver, 1995; Paulsen and Saier, 1997; Gaither and Eide, 2001; Palmiter and Huang, 2004). Thus, Msc2 is likely to be a zinc transporter whose topology is consistent with metal transport into the ER lumen. Second, mutations in *msc2* alter zinc homeostasis. Although it was shown previously that the Zap1 transcription factor was completely inactive in a zinc-limited *msc2* mutant (Li and Kaplan, 2000), our experiments further clarified these earlier results by showing that Zap1 can still respond to zinc deficiency in an *msc2* strain. Nonetheless, the suppression of ZRE-*lacZ* expression caused by the *msc2* mutation that we observed (Fig. 3) is consistent with *msc2* mutants having elevated pools of labile cytosolic zinc. Third, mutations in *MSC2* result in several phenotypes that are zinc suppressible. Li and Kaplan (2000) had shown that the growth defect of *msc2* mutants on respired carbon sources at elevated temperatures is suppressed by zinc. Here, we document that zinc-deficient cells up-regulate their UPR system and this induction is further increased in an *msc2* mutant. Like the temperature-sensitive growth phenotype, induction of the UPR is zinc suppressible. Finally, we present here genetic evidence that known zinc transporters, Zrc1 and Cot1, play redundant roles with Msc2. Their involvement in ER function indicates that Msc2 is also a zinc transporter.

Our results indicate that Msc2 delivers zinc to the lumen of the ER to maintain function of that compartment and, perhaps, other organelles of the secretory pathway. Although currently available methods do not allow us to assay lumenal ER zinc directly, several observations indirectly support this hypothesis. First, we found that Msc2 localizes to the ER when expressed at physiological levels from its own promoter. The presence of significant amounts of Msc2 protein in vesicles of lighter density (Fig. 2 A, $+Mg^{2+}$) suggests that some protein may also be found in later compartments of the secretory pathway, perhaps the Golgi. Second, mutation of *MSC2* activates the UPR system. Our results indicate that this induction requires the full UPR signaling pathway consistent with actual ER stress being responsible rather than downstream perturbations of, for example, $Hac1^{i}$ activity. Third, we found that *msc2* mutants show synthetic growth defects when combined with mutations in either *ire1* or *hac1*. This observation is especially intriguing in light of studies by Ng et al. (2000) in which mutations were identified that were synthetically lethal when combined with an *ire1* mutation. This screen identified 16 different genes almost all of which were shown to be involved in ER functions such as glycosylation, GPI anchor synthesis, or ERAD function. Thus, mutations in genes affecting lumenal ER processing events are lethal when combined with *ire1* mutations. Although *msc2* mutants were not identified in this synthetic lethal screen, they too are synthetically lethal with an *ire1* mutation when cells are grown at 37°C. Finally, we directly observed zinc-suppressible defects in one aspect of ER function, ERAD. We chose to examine this process because Scj1, a chaperone protein of the ER lumen that is required for ERAD, is likely to be zinc dependent. One caveat to this experiment is that the E3 ubiquitin-protein ligases required for proteasome degradation of unfolded proteins after their export from the ER, Hrd1/Der3, and Doa10/Ssm4, may also be zinc dependent (Bordallo and Wolf 1999; Swanson et al., 2001). Therefore, the defects in ERAD observed in *msc2* mutants could be due to disruption of ligase function via alterations in cytosolic zinc homeostasis. This

appears not to be the case; degradation of a model cytosolic substrate of Doa10, the Deg1-β-galactosidase protein (Swanson et al., 2001), was unaffected by either zinc limitation or mutation of *msc2* (unpublished data). Compromised function of Hrd1/Der3 is still formally possible but less likely given the lack of effects on Doa10 function.

In addition to ERAD, it is also likely that other processes occurring in the ER are impaired by zinc deficiency. Several observations suggest that synthesis of GPI anchors may be disrupted by these perturbations. First, GPI anchor synthesis has been found to be zinc dependent both in vitro and in vivo (Mann and Sevlever, 2001; Sevlever et al., 2001). Second, the yeast *MCD4*, *LAS21*, and *GPI13* genes encode related proteins required for GPI anchor synthesis (Gaynor et al., 1999; Tohe and Oguchi, 1999; Flury et al., 2000; Taron et al., 2000). These proteins all contain conserved domains similar to the zinc-binding sites of alkaline phosphatases (Galperin and Jedrzejas, 2001). Although the precise role of these proteins is still unclear, their importance in GPI anchor synthesis is well documented. *MCD4* and *GPI13* are essential genes whereas *LAS21* is not. Temperature-sensitive *mcd4* alleles and *las21* mutants have a large cell morphology similar to that seen with *msc2* (Mondesert et al., 1997; Li and Kaplan, 2000; Ni and Snyder, 2001). Suppressors of these mutations also link their activity to Msc2. The large cell phenotype of *las21* is suppressed by overexpression of the *HSP150* gene (Tohe and Oguchi, 1999). Hsp150 is a cell wall protein of unknown function. We have found *HSP150* overexpression also suppresses the *msc2* temperature-sensitive growth defect and large cell phenotype (unpublished data). Finally, *MCD4* is a direct Zap1 target gene and is induced greater than or equal to fourfold by zinc deficiency (Lyons et al., 2000). These results suggest that GPI anchor synthesis is sensitive to zinc deficiency, and *MCD4* is up-regulated to maintain sufficient activity in zinc-limited cells. Golgi function was unimpaired by mutation of the *MSC2* gene; analysis of the kinetics of wild-type CPY processing indicated no differences between wild-type and mutant cells in high or low zinc (unpublished data).

In this work, we have identified three different transporters that likely contribute to ER zinc: Zrc1, Cot1, and Msc2. Of these three, Msc2 appears to play the predominant role because mutation of this gene alone had the strongest effect on UPR induction. Although Msc2 is resident in the ER membrane, Zrc1 and Cot1 are most abundant in the vacuolar membrane (Li and Kaplan, 1998; MacDiarmid et al., 2002). We can suggest two possible mechanisms to explain how Zrc1 and Cot1 could supply zinc to the ER. First, these proteins may mediate zinc transport soon after insertion into the ER membrane and before their transit to the vacuole. Alternatively, zinc may be transferred from the vacuole lumen to the ER by retrograde vesicular trafficking.

The *ZRC1* gene is a Zap1 target and induced by zinc deficiency (Lyons et al., 2000; Miyabe et al., 2000). This was a surprising finding given the importance of this transporter in zinc storage and detoxification. Our previous results indicated that *ZRC1* up-regulation in low zinc is required to tolerate "zinc shock" (MacDiarmid et al., 2003). Zinc shock occurs when zinc-limited cells, which express high levels of the Zrt1 zinc uptake transporter, are resupplied with zinc. The role of Zrc1 in supplying zinc to the ER is an additional reason why the *ZRC1* gene may be induced in low zinc; i.e., to maintain ER zinc levels. However, given the relatively minor role Zrc1 plays in maintaining ER function (Fig. 8), our results argue that zinc shock tolerance is the major reason for the regulation of *ZRC1* expression by Zap1.

We also predict that additional pathways contribute to ER zinc. UPR induction in the *msc2 zrc1 cot1* triple mutant is still suppressible by adding 10 μM $ZnCl_2$ to the medium. One possible route to bypass the loss of Msc2, Zrc1, and Cot1 activity is via fluid-phase endocytosis of zinc followed by its retrograde vesicular transport to the ER. Although formally possible, we do not favor this model based on our results. Specifically, although UPR induction in the *msc2 zrc1 cot1* mutant is suppressed by 10 μM zinc, it requires 100-fold more zinc to suppress UPRE-*lacZ* activity in a *zrt1* mutant (Fig. 1 A). Zrt1 transports zinc across the plasma membrane into the cytoplasm. Therefore, the much higher levels of zinc required to suppress UPRE-*lacZ* expression in a *zrt1* mutant strongly argues that zinc must pass through the cytosol before entering the ER.

Msc2 is related to the Zhf protein of *S. pombe* (Borrelly et al., 2002; Clemens et al., 2002). Like Msc2, Zhf is a member of the CDF family of metal ion transporters. Furthermore, immunoelectron microscopy localized Zhf protein to the ER membrane. However, the phenotypic effects of *zhf* mutations argue that this protein plays a very different role in zinc metabolism. Although Msc2 is important for supplying zinc to the ER for organelle function, Zhf appears to be required for zinc storage and detoxification. For example, *zhf* mutations increase the sensitivity of cells to exogenous zinc indicating its role in detoxification. *zhf* mutants also have decreased zinc accumulation in cells indicating its role in zinc storage. For Msc2, we found no effect of *msc2* mutations on zinc tolerance either in wild-type or *zrc1 cot1* mutant cells that are greatly sensitized to exogenous zinc (unpublished data). Li and Kaplan (2000) showed that *msc2* mutants actually hyperaccumulate zinc. Thus, the effects of *zhf* mutations in *S. pombe* are much more similar to mutations altering Zrc1 and Cot1 of *S. cerevisiae*. The ER of *S. pombe* may play a role in zinc storage and detoxification similar to that of the vacuole in *S. cerevisiae*.

Another protein related to Msc2 is mammalian ZnT-5. Although most members of the CDF family have only six transmembrane domains, Msc2 and ZnT-5 are predicted to have ~15 transmembrane domains. For each, the conserved CDF region is found at the COOH terminus with several transmembrane domains attached to their NH_2 termini. ZnT-5 was localized to the Golgi when expressed from the CMV promoter in HeLa cells and is widely expressed in mammalian tissues (Kambe et al., 2002). Expression was especially high in the β cells of the pancreas in which zinc is transported into secretory vesicles for the packaging of insulin. Finally, ZnT-5–dependent zinc transport activity could be observed in Golgi-derived vesicles in vitro. Given our results indicating that zinc transport into the secretory pathway is important for ER stress and UPR induction, we predict that ZnT-5 or related proteins carry out this important

role in mammalian cells. Consistent with this hypothesis, we have found that expression of ZnT-5 in *msc2* mutant yeast can suppress phenotypic defects of this mutant under certain conditions (unpublished data).

Materials and methods

Yeast strains and growth conditions

Media used were YPD, SD, YPGE, and LZM as described previously (Gitan et al., 1998). Strains used are described in Table I. Yeast deletion mutants were obtained from Research Genetics. To generate several strains, the *KanMX* cassette with 500 bp flanking the gene to be mutated was amplified by PCR from the appropriate mutant. The PCR fragment was then transformed into the appropriate recipient strain. This method was used to generate strains CEY3-8, CEY27-29, CM158, CM160, CM162, and CM164. CM158 and CM164 were crossed to generate CEY25 and CM160 and CM162 were crossed to generate CEY26. CEY13 and CEY17 are haploid segregants of CEY25 and 26, respectively. CEY8 and DY150 were crossed to generate CEY24. CEY19-23 and CEY27-29 are haploid segregants of CEY24.

Yeast plasmids

pDg2L (ZRE-lacZ; MacDiarmid et al., 2000), pHYC3 (HIS4-lacZ; Hinnebusch et al., 1985), pMCZ-Y (UPRE-lacZ; provided by A. Cooper, University of Missouri-Kansas City; Kansas City, MO; Kawahara et al., 1997) were described previously. pSN222 (Kex2-HA) was a gift of S. Nothwehr (University of Missouri). pRK315 (Pma1-HA) was a gift of R. Kölling (Heinrich-Heine-Universität, Düsseldorf, Germany). pDN436 (CPY*–HA) was a gift of D. Ng (Pennsylvania State University, University Park, PA). pGEV-TRP was cotransformed with pRK315 so that Pma1-HA expression levels could be controlled by β-estradiol (10^{-7}M; Sigma-Aldrich) addition (Gao and Pinkham, 2000). pMCZ-YL was constructed by exchanging the *URA3* gene on pMCZ-Y with the *LEU2* gene by marker swapping (Cross, 1997). pDN436U was constructed by exchanging the *LEU2* gene on pDN436 with the *URA3* gene (Cross, 1997). To generate pMSC2, the *MSC2* ORF plus ∼500 bp of flanking DNA was amplified by PCR from genomic DNA and inserted into EcoRI-, PstI-digested pFL38 by homologous recombination (Ma et al., 1987). Msc2 function was confirmed by complementing the *msc2* mutant. To generate pMSC2HA, the *MSC2* ORF plus ∼500 bp promoter and lacking the stop codon was PCR amplified from genomic DNA and inserted into YCpZRC1-HA (MacDiarmid et al., 2002) by homologous recombination. The resulting plasmid has the *MSC2* promoter and ORF followed by three HA tags. The plasmid was confirmed by complementing the *msc2* mutant. To generate pHAC1, the *HAC1* ORF plus ∼1,300 bp upstream and ∼900 bp downstream flanking DNA were amplified from genomic DNA and inserted into SacI-, XmaI-digested pRS315 via homologous recombination. To generate pHAC1^{i}, overlap PCR was used to generate the *HAC1* ORF (plus flanking DNA as above) without the intron (Ho et al., 1989). This fragment was then inserted into pRS315 via homologous recombination. DNA sequencing confirmed the lack of the intron.

Yeast β-galactosidase assays

β-Galactosidase assays were performed on protein extracts (Ausubel et al., 1995) and specific activity was normalized to protein content.

Subcellular fractionation and immunoblotting

Subcellular fractionation was done largely as described by Roberg et al. (1997). Lysates were fractionated on 20–60% sucrose gradients prepared with 10 mM EDTA (−Mg) or with 2 mM $MgSO_4$ (+Mg). Immunoblots were done by standard techniques (Harlow and Lane, 1988). Blots were visualized with ECL (Amersham Biosciences), and band quantitation was performed using NIH Image 1.61. Antibodies used were mouse anti-HA (12CA5, Roche), rabbit anti-HA (Sigma-Aldrich), mouse anti-Dpm1 (Mo-

Table I. **Strains used in this work**

Strain	Genotype	Reference
DY150	*MATa ade2 can1 his3 leu2 trp1 ura3*	Li and Kaplan, 2000
DY150 *msc2*	DY150 *msc2::HIS3*	Li and Kaplan, 2000
DY1457	*MATα ade6 can1 his3 leu2 trp1 ura3*	Zhao and Eide, 1996a
ZHY1	DY1457 *zrt1::LEU2*	Zhao and Eide, 1996a
CM100	*MATα can1 his3 leu2 trp1 ura3*	MacDiarmid et al., 2000
CM102	CM100 *zrc1::HIS3*	MacDiarmid et al., 2000
CM103	CM100 *cot1::URA3*	MacDiarmid et al., 2000
CM104	CM100 *zrc1::HIS3 cot1::URA3*	MacDiarmid et al., 2000
CM158	CM100 *scj1::KanMX*	This work
CM160	CM100 *jem1::KanMX*	This work
CM162	DY150 *msc2::HIS3 scj1::KanMX*	This work
CM164	DY150 *msc2::HIS3 jem1::KanMX*	This work
CEY3	DY150 *ire1::KanMX*	This work
CEY4	DY150 *hac1::KanMX*	This work
CEY5	DY150 *msc2::HIS3 ire1::KanMX*	This work
CEY6	DY150 *msc2::HIS3 hac1::KanMX*	This work
CEY7	CM100 *msc2::KanMX*	This work
CEY8, 27–29	CM100 *msc2::KanMX zrc1::HIS3 cot1::URA3*	This work
CEY13	DY150 *jem1::KanMX*	This work
CEY17	DY150 *jem1::KanMX scj1::KanMX*	This work
CEY19–21	CM100 *msc2::KanMX zrc1::HIS3*	This work
CEY22, 23	CM100 *msc2::KanMX cot1::URA3*	This work
CEY24	DY150 × CEY8 diploid *MATa/α can1/can1 ade2/ADE2 his3/his3 leu2/leu2 trp1/trp1 ura3/ura3 msc2::KanMX zrc1::HIS3 cot1::URA3*	This work
CEY25	CM158 × CM164 diploid *MATa/α can1/can1 ade2/ADE2 his3/his3 leu2/leu2 trp1/trp1 ura3/ura3 msc2::HIS3 jem1::KanMX scj1::KanMX*	This work
CEY26	CM160 × CM162 diploid *MATa/α can1/can1 ade2/ADE2 his3/his3 leu2/leu2 trp1/trp1 ura3/ura3 msc2::HIS3 jem1::KanMX scj1::KanMX*	This work

lecular Probes), mouse anti-Pgk1 (Molecular Probes), goat anti–mouse HRP-conjugated secondary (Pierce Chemical Co.), and goat anti–rabbit HRP-conjugated secondary (Pierce Chemical Co.).

Assay of ERAD

Yeast were grown in 200-ml cultures to an $OD_{600} = \sim 0.5$. Cells were harvested and resuspended in 100 ml of fresh media to a final $OD_{600} = \sim 1.0$. Cells were grown 30 min, then cycloheximide (Sigma-Aldrich) was added to a final concentration of 100 μg/ml. 5 ml aliquots of cells were removed at each time point to tubes containing NaN_3 to a final concentration of 10 mM. After the last time point, the cells were collected by centrifugation and washed once with cold buffer containing 10 mM NaN_3, 1 mM EDTA. Cells were resuspended in 1 ml of the same buffer and transferred to microfuge tubes. Cells were pelleted and resuspended in 200 μl cold protein extraction buffer (10 mM Tris-Cl, pH 8, 25 mM ammonium acetate, 1 mM EDTA, 1 mM PMSF, 10% trichloroacetic acid [Sigma-Aldrich], yeast proteinase inhibitor cocktail [complete mini EDTA-free pellets; Roche]). An equal volume of glass beads was added and the tubes were vortexed five times for 1 min, with 1 min on ice between pulses. Lysates were transferred to fresh tubes. Another 500 μl of protein extraction buffer was added to the glass beads, vortexed 1 min, and then pooled with the previous lysates. Lysates were centrifuged at 14,000 *g* at 4°C for 10 min. The supernatant was removed and discarded. The pellets were resuspended in 120 μl buffer I (100 mM Tris base, 3% SDS, 1 mM PMSF), then boiled for 5 min. Insoluble debris was pelleted by centrifuging 5 min at 15,800 *g*. The supernatant was transferred to new tubes and protein concentrations were measured using the DC protein kit (Bio-Rad Laboratories). 10 μg of protein were loaded per lane when analyzed by immunoblotting.

Cell culture, transient transfection, mammalian plasmids, and assays

HeLa cells were cultured in DME (Invitrogen) plus 0.45% glucose under 5% CO_2. All media contained 100 U/ml penicillin, 100 μg/ml streptomycin, 2 mM L-glutamine, and 100 μM MEM nonessential amino acids (Invitrogen) supplemented with 10% FBS (Invitrogen). p5xATF6GL3 was a gift of R. Prywes (Columbia University, New York, NY), and contains five repeats of an ATF6 binding site cloned into a minimal promoter preceding the firefly luciferase gene (Wang et al., 2000). pSV-β-galactosidase control vector (Promega) was used as a control for transfection efficiency. HeLa cells ($\sim 1.2 \times 10^6$) were seeded in 60-mm plates and transiently transfected using Lipofectamine 2000 (Invitrogen). Both p5xATF6GL3 and pSV-β-galactosidase plasmids were cotransfected in all experiments. Transfection efficiencies were typically 60%. 36–48 h after transfection, tunicamycin (Sigma-Aldrich), $ZnCl_2$, or TPEN (Sigma-Aldrich) was added to the culture media at the indicated concentrations. After treatment, the cells were washed three times with cold PBS. To generate protein extracts and perform luciferase and β-galactosidase assays, the luciferase assay system with reporter lysis buffer (Promega) was used. Luciferase activity was normalized to β-galactosidase activity as an internal control.

The authors thank J. Kaplan (Table I, strains DY150 and DY150msc2; University of Utah, Salt Lake City, Utah), A. Cooper, S. Nothwehr, R. Prywes, and D. Ng for providing strains and/or plasmids and W. Folk for use of his luminometer.

This work was supported by National Institutes of Health grants GM56285 and GM69786. C.D. Ellis was supported by an MU Life Sciences Predoctoral Fellowship.

Submitted: 30 January 2004
Accepted: 9 June 2004

References

Ausubel, F.M., R. Brent, R.E. Kingston, D.D. Moore, J.G. Seidman, J.A. Smith, and K. Struhl. 1995. β-Galactosidase assays. *In* Current Protocols in Molecular Biology. John Wiley & Sons Inc., New York, NY. 13.6.1–13.6.5.

Bordallo, J., and D.H. Wolf. 1999. A RING-H2 finger motif is essential for the function of Der3/Hrd1 in endoplasmic reticulum associated protein degradation in the yeast *Saccharomyces cerevisiae*. *FEBS Lett.* 448:244–248.

Borrelly, G.P., M.D. Harrison, A.K. Robinson, S.G. Cox, N.J. Robinson, and S.K. Whitehall. 2002. Surplus zinc is handled by Zym1 metallothionein and Zhf endoplasmic reticulum transporter in *Schizosaccharomyces pombe*. *J. Biol. Chem.* 277:30394–30400.

Chang, C., and Z. Werb. 2001. The many faces of metalloproteases: cell growth, invasion, angiogenesis and metastasis. *Trends Cell Biol.* 11:S37–S43.

Clemens, S., T. Bloss, C. Vess, D. Neumann, D.H. Nies, and U. Zur Nieden. 2002. A transporter in the endoplasmic reticulum of *Schizosaccharomyces pombe* cells mediates zinc storage and differentially affects transition metal tolerance. *J. Biol. Chem.* 277:18215–18221.

Cross, F.R. 1997. "Marker swap" plasmids: convenient tools for budding yeast molecular genetics. *Yeast.* 13:647–653.

Dodson, G., and D. Steiner. 1998. The role of assembly in insulin's biosynthesis. *Curr. Opin. Struct. Biol.* 8:189–194.

Finger, A., M. Knop, and D.H. Wolf. 1993. Analysis of two mutated vacuolar proteins reveals a degradation pathway in the endoplasmic reticulum or a related compartment of yeast. *Eur. J. Biochem.* 218:565–574.

Flury, I., A. Benachour, and A. Conzelmann. 2000. YLL031c belongs to a novel family of membrane proteins involved in the transfer of ethanolaminephosphate onto the core structure of glycosylphosphatidylinositol anchors in yeast. *J. Biol. Chem.* 275:24458–24465.

Gaither, L.A., and D.J. Eide. 2001. Eukaryotic zinc transporters and their regulation. *Biometals.* 14:251–270.

Galperin, M.Y., and M.J. Jedrzejas. 2001. Conserved core structure and active site residues in alkaline phosphatase superfamily enzymes. *Proteins.* 45:318–324.

Gao, C.Y., and J.L. Pinkham. 2000. Tightly regulated, beta-estradiol dose-dependent expression system for yeast. *Biotechniques.* 29:1226–1231.

Gaynor, E.C., G. Mondesert, S.J. Grimme, S.I. Reed, P. Orlean, and S.D. Emr. 1999. *MCD4* encodes a conserved endoplasmic reticulum membrane protein essential for glycosylphosphatidylinositol anchor synthesis in yeast. *Mol. Biol. Cell.* 10:627–648.

Gitan, R.S., H. Luo, J. Rodgers, M. Broderius, and D. Eide. 1998. Zinc-induced inactivation of the yeast ZRT1 zinc transporter occurs through endocytosis and vacuolar degradation. *J. Biol. Chem.* 273:28617–28624.

Grass, G., B. Fan, B.P. Rosen, S. Franke, D.H. Nies, and C. Rensing. 2001. ZitB (YbgR), a member of the cation diffusion facilitator family, is an additional zinc transporter in *Escherichia coli*. *J. Bacteriol.* 183:4664–4667.

Harding, H.P., M. Calfon, F. Urano, I. Novoa, and D. Ron. 2002. Transcriptional and translational control in the mammalian unfolded protein response. *Annu. Rev. Cell Dev. Biol.* 18:575–599.

Harlow, E., and D. Lane. 1988. Immunoblotting: Antibodies. *In* A Laboratory Manual. Cold Spring Harbor Press, Cold Spring Harbor, New York. 471–510.

Hinnebusch, A.G., G. Lucchini, and G.R. Fink. 1985. A synthetic *HIS4* regulatory element confers general amino acid control on the cytochrome c gene (*CYC1*) of yeast. *Proc. Natl. Acad. Sci. USA.* 82:498–502.

Ho, S.N., H.D. Hunt, R.M. Horton, J.K. Pullen, and L.R. Pease. 1989. Site-directed mutagenesis by overlap extension using the polymerase chain reaction. *Gene.* 77:51–59.

Huang, L., C.P. Kirschke, and J. Gitschier. 2002. Functional characterization of a novel mammalian zinc transporter, ZnT6. *J. Biol. Chem.* 277:26389–26395.

Huang, X.F., and P. Arvan. 1995. Intracellular transport of proinsulin in pancreatic β-cells. *J. Biol. Chem.* 270:20417–20423.

Kambe, T., H. Narita, Y. Yamaguchi-Iwai, J. Hirose, T. Amano, N. Sugiura, R. Sasaki, K. Mori, T. Iwanaga, and M. Nagao. 2002. Cloning and characterization of a novel mammalian zinc transporter, zinc transporter 5, abundantly expressed in pancreatic beta cells. *J. Biol. Chem.* 277:19049–19055.

Kamizono, A., M. Nishizawa, Y. Teranishi, K. Murata, and A. Kimura. 1989. Identification of a gene conferring resistance to zinc and cadmium ions in the yeast *Saccharomyces cerevisiae*. *Mol. Gen. Genet.* 219:161–167.

Kang, T., H. Nagase, and D. Pei. 2002. Activation of membrane-type matrix metalloproteinase 3 zymogen by the proprotein convertase furin in the trans-Golgi network. *Cancer Res.* 62:675–681.

Kawahara, T., H. Yanagi, T. Yura, and K. Mori. 1997. Endoplasmic reticulum stress-induced mRNA splicing permits synthesis of transcription factor Hac1p/Ern4p that activates the unfolded protein response. *Mol. Biol. Cell.* 8:1845–1862.

Kirschke, C.P., and L. Huang. 2003. ZnT7, A novel mammalian zinc transporter, accumulates zinc in the Golgi apparatus. *J. Biol. Chem.* 278:4096–4102.

Kobayashi, T., M. Beuchat, M. Lindsay, S. Frias, R.D. Palmiter, H. Sakuraba, R.G. Parton, and J. Gruenberg. 1999. Late endosomal membranes rich in lysobisphosphatidic acid regulate cholesterol transport. *Nat. Cell Biol.* 1:113–118.

Li, L., and J. Kaplan. 1997. Characterization of two homologous yeast genes that encode mitochondrial iron transporters. *J. Biol. Chem.* 272:28485–28493.

Li, L., and J. Kaplan. 1998. Defects in the yeast high affinity iron transport system result in increased metal sensitivity because of the increased expression of transporters with a broad transition metal specificity. *J. Biol. Chem.* 273:

22181–22187.

Li, L., and J. Kaplan. 2000. The yeast gene *MSC2*, a member of the cation diffusion facilitator family, affects the cellular distribution of zinc. *J. Biol. Chem.* 276:5036–5043.

Linke, K., T. Wolfram, J. Bussemer, and U. Jakob. 2003. The roles of the two zinc binding sites in DnaJ. *J. Biol. Chem.* 278:44457–44466.

Lyons, T.J., A.P. Gasch, L.A. Gaither, D. Botstein, P.O. Brown, and D.J. Eide. 2000. Genome-wide characterization of the Zap1p zinc-responsive regulon in yeast. *Proc. Natl. Acad. Sci. USA.* 97:7957–7962.

Ma, H., S. Kunes, P.J. Schatz, and D. Botstein. 1987. Plasmid construction by homologous recombination in yeast. *Gene.* 58:201–216.

MacDiarmid, C.W., L.A. Gaither, and D. Eide. 2000. Zinc transporters that regulate vacuolar zinc storage in *Saccharomyces cerevisiae. EMBO J.* 19:2845–2855.

MacDiarmid, C.W., M.A. Milanick, and D.J. Eide. 2002. Biochemical properties of vacuolar zinc transport systems of *Saccharomyces cerevisiae. J. Biol. Chem.* 277:39187–39194.

MacDiarmid, C.W., M.A. Milanick, and D.J. Eide. 2003. Induction of the *ZRC1* metal tolerance gene in zinc-limited yeast confers resistance to zinc shock. *J. Biol. Chem.* 278:15065–15072.

Mann, K.J., and D. Sevlever. 2001. 1,10-Phenanthroline inhibits glycosylphosphatidylinositol anchoring by preventing phosphoethanolamine addition to glycosylphosphatidylinositol anchor precursors. *Biochemistry.* 40:1205–1213.

Miyabe, S., S. Izawa, and Y. Inoue. 2000. Expression of *ZRC1* coding for suppressor of zinc toxicity is induced by zinc-starvation stress in Zap1-dependent fashion in *Saccharomyces cerevisiae. Biochem. Biophys. Res. Commun.* 276: 879–884.

Miyabe, S., S. Izawa, and Y. Inoue. 2001. Zrc1 is involved in zinc transport system between vacuole and cytosol in *Saccharomyces cerevisiae. Biochem. Biophys. Res. Commun.* 282:79–83.

Mondesert, G., D.J. Clarke, and S.I. Reed. 1997. Identification of genes controlling growth polarity in the budding yeast *Saccharomyces cerevisiae*: a possible role of N-glycosylation and involvement of the exocyst complex. *Genetics.* 147:421–434.

Ng, D.T., E.D. Spear, and P. Walter. 2000. The unfolded protein response regulates multiple aspects of secretory and membrane protein biogenesis and endoplasmic reticulum quality control. *J. Cell Biol.* 150:77–88.

Ni, L., and M. Snyder. 2001. A genomic study of the bipolar bud site selection pattern in *Saccharomyces cerevisiae. Mol. Biol. Cell.* 12:2147–2170.

Nies, D.H., and S. Silver. 1995. Ion efflux systems involved in bacterial metal resistances. *J. Ind. Microbiol.* 14:186–199.

Nishikawa, S., and T. Endo. 1997. The yeast JEM1p is a DnaJ-like protein of the endoplasmic reticulum membrane required for nuclear fusion. *J. Biol. Chem.* 272:12889–12892.

Nishikawa, S.I., S.W. Fewell, Y. Kato, J.L. Brodsky, and T. Endo. 2001. Molecular chaperones in the yeast endoplasmic reticulum maintain the solubility of proteins for retrotranslocation and degradation. *J. Cell Biol.* 153:1061–1070.

Palmiter, R.D., and S.D. Findley. 1995. Cloning and functional characterization of a mammalian zinc transporter that confers resistance to zinc. *EMBO J.* 14: 639–649.

Palmiter, R.D., and L. Huang. 2004. Efflux and compartmentalization of zinc by members of the SLC30 family of solute carriers. *Pflugers Arch.* 447:744–751.

Palmiter, R.D., T.B. Cole, and S.D. Findley. 1996. ZnT-2, a mammalian protein that confers resistance to zinc by facilitating vesicular sequestration. *EMBO J.* 15:1784–1791.

Patil, C., and P. Walter. 2001. Intracellular signaling from the endoplasmic reticulum to the nucleus: the unfolded protein response in yeast and mammals. *Curr. Opin. Cell Biol.* 13:349–355.

Paulsen, I.T., and M.H. Saier. 1997. A novel family of ubiquitous heavy metal ion transport proteins. *J. Membr. Biol.* 156:99–103.

Pei, D., and S.J. Weiss. 1995. Furin-dependent intracellular activation of the human stromelysin-3 zymogen. *Nature.* 375:244–247.

Roberg, K.J., N. Rowley, and C.A. Kaiser. 1997. Physiological regulation of membrane protein sorting late in the secretory pathway of *Saccharomyces cerevisiae. J. Cell Biol.* 137:1469–1482.

Sevlever, D., K.J. Mann, and M.E. Medof. 2001. Differential effect of 1,10-phenanthroline on mammalian, yeast, and parasite glycosylphosphatidylinositol anchor synthesis. *Biochem. Biophys. Res. Commun.* 288:1112–1118.

Shulga, N., N. Mosammaparast, R. Wozniak, and D.S. Goldfarb. 2000. Yeast nucleoporins involved in passive nuclear envelope permeability. *J. Cell Biol.* 149:1027–1038.

Silberstein, S., G. Schlenstedt, P.A. Silver, and R. Gilmore. 1998. A role for the DnaJ homologue Scj1p in protein folding in the yeast endoplasmic reticulum. *J. Cell Biol.* 143:921–933.

Swanson, R., M. Locher, and M. Hochstrasser. 2001. A conserved ubiquitin ligase of the nuclear envelope/endoplasmic reticulum that functions in both ER-associated and Matα2 repressor degradation. *Genes Dev.* 15:2660–2674.

Tang, W., and C. Wang. 2001. Zinc fingers and thiol-disulfide oxidoreductase activities of chaperone DnaJ. *Biochemistry.* 40:14985–14994.

Taron, C.H., J.M. Wiedman, S.J. Grimme, and P. Orlean. 2000. Glycosylphosphatidylinositol biosynthesis defects in Gpi11p- and Gpi13p-deficient yeast suggest a branched pathway and implicate gpi13p in phosphoethanolamine transfer to the third mannose. *Mol. Biol. Cell.* 11:1611–1630.

Thompson, D.A., and F.W. Stahl. 1999. Genetic control of recombination partner preference in yeast meiosis: isolation and characterization of mutants elevated for meiotic unequal sister-chromatid recombination. *Genetics.* 153: 621–641.

Tohe, A., and T. Oguchi. 1999. Las21 participates in extracellular/cell surface phenomena in *Saccharomyces cerevisiae. Genes Genet. Syst.* 74:241–256.

Travers, K.J., C.K. Patil, L. Wodicka, D.J. Lockhart, J.S. Weissman, and P. Walter. 2000. Functional and genomic analyses reveal an essential coordination between the unfolded protein response and ER-associated degradation. *Cell.* 101:249–258.

Wang, Y., J. Shen, N. Arenzana, W. Tirasophon, R.J. Kaufman, and R. Prywes. 2000. Activation of ATF6 and an ATF6 DNA binding site by the endoplasmic reticulum stress response. *J. Biol. Chem.* 275:27013–27020.

Waters, B.M., and D.J. Eide. 2002. Combinatorial control of yeast *FET4* gene expression in response to iron, zinc, and oxygen. *J. Biol. Chem.* 277:33749–33757.

Zhao, H., and D. Eide. 1996a. The yeast *ZRT1* gene encodes the zinc transporter of a high affinity uptake system induced by zinc limitation. *Proc. Natl. Acad. Sci. USA.* 93:2454–2458.

Zhao, H., and D. Eide. 1996b. The *ZRT2* gene encodes the low affinity zinc transporter in *Saccharomyces cerevisiae. J. Biol. Chem.* 271:23203–23210.

Zhao, H., and D.J. Eide. 1997. Zap1p, a metalloregulatory protein involved in zinc-responsive transcriptional regulation in *Saccharomyces cerevisiae. Mol. Cell. Biol.* 17:5044–5052.

Zhao, H., E. Butler, J. Rodgers, T. Spizzo, and S. Duesterhoeft. 1998. Regulation of zinc homeostasis in yeast by binding of the ZAP1 transcriptional activator to zinc-responsive promoter elements. *J. Biol. Chem.* 273:28713–28720.